Volcanic Disruption of the Equatorial Ionosphere: ICON Observations of the Tonga Eruption

L. Claire Gasque[1], Thomas J. Immel[1] , Brian J. Harding[1], Yen-Jung J. Wu[1], Colin C. Triplett[1]

[1] Space Sciences Lab, University of California, Berkeley

Ionospheric Impacts of Volcanic Eruptions

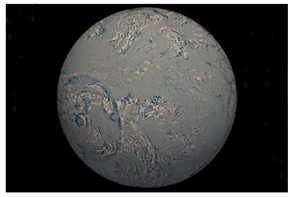

Fig 1: NOAA GOES-West satellite imagery reveals a global atmospheric pressure wave launched by the Tonga eruption. (Credit: Mathew Barlow/U Mass Lowell)

The Hunga Tonga-Hunga Ha'apai (hereafter called 'Tonga') volcano erupted at ~4:15UT on 1/15/22, driving atmospheric pressure waves around the globe [1,2] (Fig 1). These waves propagated into space, producing traveling ionospheric disturbances (TIDs) [3,4,5] which persisted for several days after the eruption [6]. While direct modification of the ionosphere has been associated with the passage of atmospheric waves originating in the lower atmosphere [7], the potentially larger electrodynamic effects on the plasma have only recently been considered [8]. **Here we show immediate, global-scale dynamo effects of the eruption using observations from NASA's Ionospheric Connection Explorer (ICON).**

Data and Methods

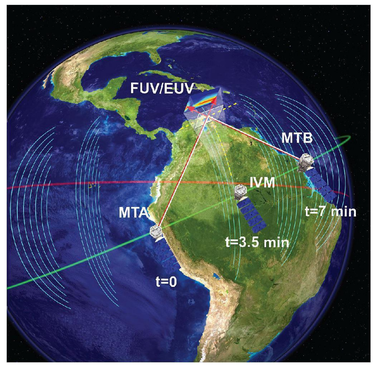

Fig 2: ICON instruments and observing geometry (credit: UCB/SSL)

The ICON mission explores energy and momentum transfer from solar and atmospheric sources into the ionosphere [9], so is apt to study Tonga's ionospheric effects. ICON's Ion Velocity Meter (IVM) measures in situ plasma densities and drifts [10], MIGHTI remote-senses neutral wind profiles [11], and the Far Ultra-Violet (FUV) Imager remote-senses plasma density profiles [12] (Fig. 2). For the relevant scale sizes (>1s, >10km), IVM measurements can be extrapolated along the field lines, providing remote sampling of the electric field.

To distinguish from quiet-time variability, we find the solar local time-dependent ion drift climatology for Jan 8-13, 2022 (gray in Fig. 4c), when magnetic conditions were quiet (Fig 3). We omit the day before the eruption due to a geomagnetic storm. As noted by Harding et al. (2022) [8], there is little evidence of penetration electric fields due to the storm, so it is unlikely to confound our analysis.

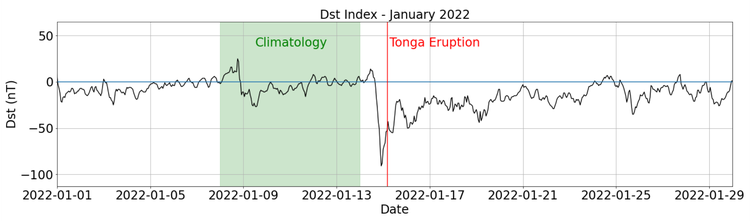

Fig 3: Disturbance Storm Time (Dst) Index (https://wdc.kugi.kyoto-u.ac.jp/dstdir/) for Jan. 2022. The relatively quiet period over which we evaluated the climatology is highlighted in green

Observations: ICON's First Glimpse of the Eruption

We report extreme zonal and vertical ExB ion drifts (6.9σ and 8.8σ w.r.t to the climatology, respectively) ~4000 km away from Tonga within an hour of the eruption, well before the arrival of any atmospheric wave (Fig 4).

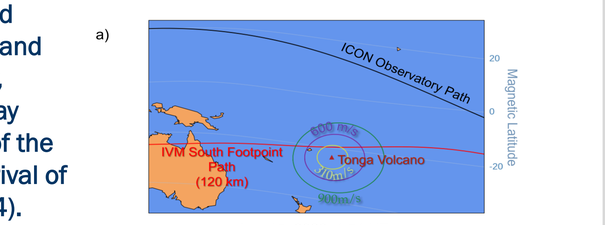

Fig 4: a) ICON's location and magnetic footprint for its first orbit post-eruption, including wavefronts of disturbances traveling at 900m/s (green), 600m/s (purple), and 310m/s (yellow, representing a Lamb wave). b) The magnetic field line connected to ICON at its closest approach to Tonga. A simple spherical wavefront model shows that when the south magnetic footprint is north of the volcano the neutral wind is expected to be mostly northward, driving a westward ExB ion drift. c) IVM meridional and zonal drift measurements during ICON's first Tonga encounter. The climatologies are shown in gray (dark gray line: median; dark gray region: 25th-75th quantiles; light gray region: 10th-90th quantiles). Notice the extreme vertical and zonal drifts within the region affected by a 600m/s wavefront driven by the volcano.

Theory: Disruptions to the E-Region Dynamo

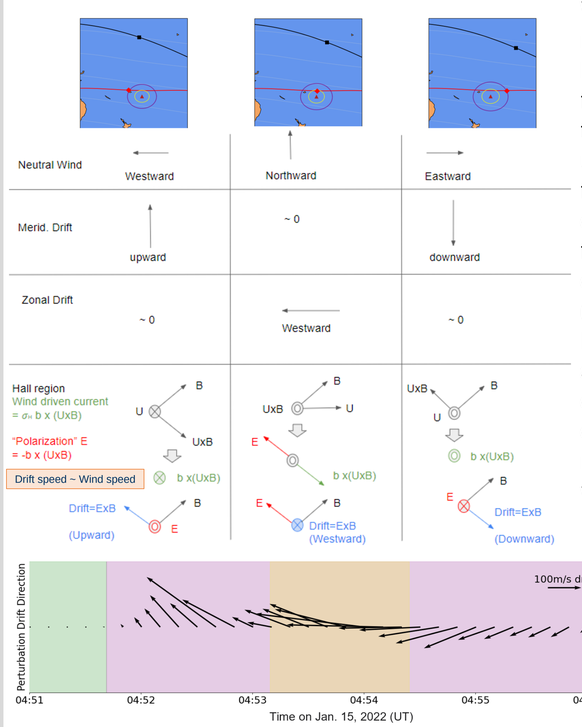

With a spherically expanding neutral wind model (Fig 4b), the IVM south footpoint encounters first a westward, then northward, then eastward wind (Fig 5). We use a simplified slab model following Kelley 2009 [13] to determine the resulting electric fields and ion drifts, considering currents in only the Hall region (~100-120km) and neglecting Pedersen currents. In this model, a polarization electric field is created to balance the wind-driven current and find the resulting ExB drifts, which agree well with our observations.

Fig 5: Theoretical predictions from a spherical neutral wind and simplified slab model of Hall region currents driving the ionospheric dynamo. The chart shows the expected neutral wind input and the resulting predictions of vertical and zonal drifts. The final panel shows perturbation drifts derived from the observations in Fig 4c. The observations are consistent with theoretically predicted drifts.

Discussion and Conclusions

The region with extreme ion drifts was magnetically connected to the E-region just 400km from Tonga, **suggesting that the wavefront expanding from Tonga created strong electric potentials which were then transmitted along the magnetic field (i.e., via Alfvén waves).** A simple theoretical model (Fig. 5) reveals that the observed drift signatures are consistent with an expanding wave with a large (>200m/s) neutral wind amplitude. **These observations are the first direct detection in space of the near-immediate dynamo effects of a volcanic eruption and will prove essential for constraining ionospheric models of impulsive lower atmospheric events.**

Ongoing Work: ICON's Later Tonga Encounters

This work examined Tonga's immediate dynamo effects, studying ICON's first orbit post-eruption, when only the IVM sampled the region affected by the volcano. **Ongoing work will examine ICON's later orbits, incorporating neutral wind and density profile data to get a more complete picture of how the eruption's ionospheric dynamo modification evolves.**

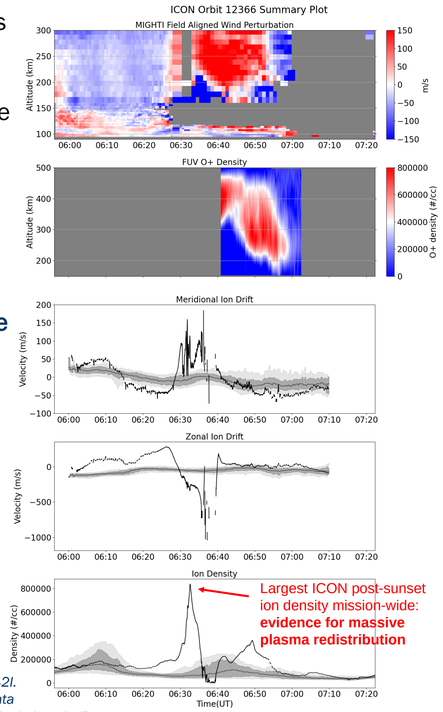

Fig 6: Summary plot of ICON's second orbit following the eruption, including neutral wind perturbation and O+ density profile, as well as IVM ion drifts and density. Notice the extreme field-aligned winds, as well as the large increase followed by complete drop out in the density. Future work will interpret data from this and later orbits.

Acknowledgements and References

ICON is supported by NASA's Explorers Program through contracts NNG12FA45C and NNG12FA42I. ICON data are processed in the ICON Science Data Center at UCB and available at https://icon.ssl.berkeley.edu/Data.

[1] A. Amores, S. Monserrat, M. Marcos, D. Argüeso, J. Villalonga, G. Jordà, and D. Gomis. "Numerical simulation of atmospheric lamb waves generated by the 2022 hunga-tonga volcanic eruption." Geophysical Research Letters, page e2022GL098240, 2022.

[2] C. Wright, N. Hindley, M. J. Alexander, M. Barlow, L. Hoffmann, C. Mitchell, F. Prata, M. Bouillon, J. Carstens, C. Clerbaux, et al. "Tonga eruption triggered waves propagating globally from surface to edge of space." 2022.

[3] E. Aa, S.-R. Zhang, P. J. Erickson, J. Vierinen, A. J. Coster, L. P. Goncharenko, A. Spicher, and W. Rideout. "Significant equatorial plasma bubbles and global ionospheric disturbances after the 2022 tonga volcano eruption." Earth and Space Science Open Archive, page 17, 2022.

[4] J.-T. Lin, P. K. Rajesh, C. C. Lin, M.-Y. Chou, J.-Y. Liu, J. Yue, T.-Y. Hsiao, H.-F. Tsai, H.-M. Chao, and M.-M. Kung. "Rapid conjugate appearance of the giant ionospheric lamb wave in the northern hemisphere after hunga-tonga volcano eruptions." 2022.

[5] D. R. Themens, C. Watson, N. Žagar, S. Vasylkevych, S. Elvidge, A. McCaffrey, P. Prikryl, B. Reid, A. Wood, and P. Jayachandran. "Global propagation of ionospheric disturbances associated with the 2022 tonga volcanic eruption." Geophysical Research Letters, page e2022GL098158, 2022.

[6] S.-R. Zhang, J. Vierinen, E. Aa, L. Goncharenko, P. Erickson, W. Rideout, A. Coster, and A. Spicher. 2022 tonga volcanic eruption induced global propagation of ionospheric disturbances via lamb waves. 2022.

[7] E. Astafyeva. Ionospheric detection of natural hazards. Reviews of Geophysics, 57(4):1265–1288, 2019.

[8] B. J. Harding, Y.-J. J. Wu, P. Alken, Y. Yamazaki, C. Triplett, T. J. Immel, L. C. Gasque, S. B. Mende, and C. Xiong. "Impacts of the january 2022 tonga volcanic eruption on the ionospheric dynamo: Icon-mighti and swarm observations of extreme neutral winds and currents." 2022.

[9] T. J. Immel, S. England, S. Mende, R. Heelis, C. Englert, J. Edelstein, H. Frey, E. Korpela, E. Taylor, W. Craig, et al. The ionospheric connection explorer mission: mission goals and design. Space Science Reviews, 214(1):1–36, 2018.

[10] R. Heelis, R. Stoneback, M. Perdue, M. Depew, W. Morgan, M. Mankey, C. Lippincott, L. Harmon, and B. Holt. Ion velocity measurements for the ionospheric connections explorer. Space science reviews, 212(1):615–629, 2017.

[11] C. R. Englert, J. M. Harlander, C. M. Brown, K. D. Marr, I. J. Miller, J. E. Stump, J. Hancock, J. Q. Peterson, J. Kumler, W. H. Morrow, et al. Michelson interferometer for global high-resolution thermospheric imaging (mighti): instrument design and calibration. Space science reviews, 212(1):553–584, 2017.

[12] S. Mende, H. Frey, K. Rider, C. Chou, S. Harris, O. Siegmund, S. England, C. Wilkins, W. Craig, T. Immel, et al. The far ultra-violet imager on the icon mission. Space Science Reviews, 212(1):655–696, 2017.

[13] M. C. Kelley. The Earth's ionosphere: plasma physics and electrodynamics. Academic press, 2009.